Scientific Journal for Damietta Faculty of Science **13**(3) 2023, 79-87
doi: 10.21608/SJDFS.2023.242279.1136
ISSN Print 2314-8594
ISSN Online 2314-8616

https://sjdfs.journals.ekb.eg/

Biological Synthesis and Characterization of Antibacterial Manganese Oxide Nanoparticles using Bacillus Subtilis ATCC6633

Abdallah A.Z El-Zahed[1], Mahmoud E. Khalifa[1], Mohamed M. El-Zahed[*1] and Zakaria A. Baka[1]

[1]Botany and Microbiology department , Faculty of science, Damietta University, Egypt.

Received: 12 October 2023 /Accepted: 25 October 2023

[*] Corresponding author's E-mail: Mohamed.marzouq91@du.edu.eg

Abstract

Green synthesis sources for synthesizing metal oxide nanoparticles are an interesting and expanding research area due to their potential antibacterial applications. Generally, nanoparticles are prepared using different chemical and physical methods that yield toxic or harmful nano-scaled particles in addition to the high cost and complicated processing steps. The present study successfully biosynthesized manganese oxide nanoparticles (MnO NPs) by reducing Manganese sulfate **(**$MnSO_4.H_2O$) using the cell-free supernatant of *Bacillus subtilis* ATCC6633. The formation of MnO NPs was confirmed by UV-Vis spectroscopy, Fourier-transform infrared spectroscopy (FT-IR), Zeta analysis and transmission electron microscope (TEM). The biosynthesized MnO NPs displayed two absorption peaks at 285 and 353 nm. FT-IR spectrum proved the existence of bacterial proteins during the biosynthesis of MnO NPs that might act as stabilizing agents. MnO NPs have a negative charge of -20.4 mV according to Zeta analysis. TEM micrographs showed the rod-shape of MnO NPs with lengths of 70 to 100 nm and diameters of 10 to 23 nm. MnO NPs had a bactericidal action against *Bacillus cereus* and *Escherichia coli* with zones of inhibition of 23 and 25 mm, respectively in addition to minimum inhibitory concentration values of 20 and 15 µg/ml, respectively. The obtained results highlighted the possibility of using MnO NPs as a strong antibacterial agent in different industrial and medical applications.

Keywords: Manganese oxide, nanoparticles, biological synthesis, characterization, antibacterial activity.

Introduction

Chemistry, engineering sciences, physics, and materials sciences are all combined in the multidisciplinary field of nanotechnology (Omran, 2020). Designing, synthesising, characterising, and producing nanoscaled materials with precise forms and sizes is the fundamental goal of this branch of study. It deals with substances that are less than 100 nm in size. Nano is a Latin word that means 'Dwarf 'and the thought of nanotechnology was first time given by Nobel laureate physics Richard Fenman in South California in 1952 (Buzea et al., 2007). In a real sense term nanotechnology was popularized by Eric Drexlerin the 1980s

(Verma et al., 2012). Nanomaterials, nanoparticles (NPs), nanocomposites, and nanostructures are all terms used to describe these substances. These materials have exceptional functional, magnetic, optical, electrical, and mechanical properties (Silva, 2004). Many applications use the NPs as antimicrobial, anticancer, antioxidant and environmental remediation agents (Kakade, 2003). Some metal and metal oxide NPs showed strong antimicrobial effects against different bacterial strains including *Bacillus* sp., *Escherichia coli*, *Staphylococcus aureus* and *Pseudomonas aeruginosa* (Gopinath et al., 2012; Khan & Bano, 2016a, 2016b). Manganese oxide nanoparticles (MnO NPs) among NPs have attracted a lot of interest in a number of domains, including antibacterial activities, therapies, bio-molecular detection, manganese (Mn) nanocoated medical devices, and optical receptor (Bar et al., 2009; Bhattacharya & Mukherjee, 2008; Li et al., 2011; Velusamy et al., 2016).

In the field of nanotechnology, the creation of NPs is a crucial step (Kannan et al., 2010). Several methods have been reported to create MnO NPs, including freeze-drying (Shaik et al., 2019), solvothermal (Shukla et al., 2015), co-precipitation (Ranjan et al., 2015), hydrothermal (Reddy & Reddy, 2003), and sol-gel (Raj et al., 2015). According to top-down and bottom-up methods, the fundamental synthesis principles of MnO NPs can be divided into two groups (Salavati-Niasari et al., 2008; Yang et al., 2022). Chemical and physical synthesis frequently employ the top-down approach (Dawadi et al., 2020; Naseri et al., 2011). The top-down technique is not frequently used because of the high preparation costs and structural flaws in generated NPs (Nikam et al., 2018). On the other hand, the green synthesis of MnO NPs is frequently described as using bottom-up synthesis techniques (Hoseinpour & Ghaemi, 2018). All of these strategies for the synthesis of NPs have been documented (Enriquez-Sánchez et al., 2020; Narayanan & Sakthivel, 2010; Pinc et al., 2017). They all involve the use of hazardous chemicals and high-energy physical processes. Chemical production of MnO NPs involves the use of redox and microemulsion methods. This approach has advantages including a quicker synthesis time, less energy loss, and the capacity to produce more MnO NPs. Toxic and dangerous compounds are, however, added to this procedure throughout the synthesis process (Ali et al., 2019; Jin et al., 2015). Overcoming the limitations of traditional methods, green synthesis-sources for synthesizing NPs have emerged (Grasso et al., 2019). Additionally, the biological approach, particularly the use of natural organisms, is an economical, easy-to-use, non-toxic, and environmentally acceptable strategy. The green synthesis of metal and metal oxide NPs mostly uses plants and microorganisms, such as bacteria, fungi, yeast, and algae. In contrast to conventional chemical and physical techniques, the biosynthesis of nanomaterials by microorganisms is gaining attention as a novel, interesting method for the development of "greener" nanomanufacturing. The current study therefore emphasised the biological production of MnO NPs utilising *Bacillus subtilis* ATCC6633 as a biological reducing agent. Gram-negative and Gram-positive bacteria were examined for their susceptibility to the biosynthesized MnO NPs.

Materials and Methods

Microbial strains

American Type Culture Collection (ATCC) bacterial strains: *Bacillus subtilis* ATCC6633, *B. cereus* ATCC 14579 and *E. coli* ATCC25922 were obtained from the Botany and Microbiology Department, Faculty of Science, Damietta University, Egypt.

Manganese (II) sulfate **(**$MnSO_4.H_2O$) was purchased from Sigma Aldrich, USA.

Extracellular biosynthesis of MnO NPs using B. subtilis ATCC6633

In nutrient broth flasks, *B. subtilis* ATCC6633 was grown aerobically at 150 rpm and 37 °C. Centrifuging the bacterial culture at 5000 rpm for 15 minutes produced the bacterial metabolite. 0.1 M MnSO4 in an aqueous solution. The bacterial metabolite was produced, and 40:1 volume of water was added. When the pH reached 8, the mixture was gradually and continuously stirred (at 200 rpm) with drops of 5 M NaOH solution. A magnetic stirrer was used to agitate the mixture for two minutes at 60 °C. The mixture was centrifuged for 10 minutes at 5000 rpm; the supernatant was then discarded. All the synthesised MnO NPs were dried in an oven at 50°C after being rinsed

four times with distilled water for additional characterisation and antibacterial tests.

Characterization of the biosynthesized MnO NPs

UV-visible spectrophotometer (UV-Vis spectrophotometer V-760, JASCO, UK) and Fourier-transform infrared spectroscopy (FT-IR) spectrometer (FT/IR-4000 Series JASCO, UK) were used for a spectral study of MnO NPs. Zeta potential analysis (Malvern Zetasizer Nano-ZS90, UK) was applied to measure the charge of MnO NPs. transmission electron microscope (TEM, JEOL JEM-2100, Japan) was used to study the size and morphology of the MnO NPs.

Antibacterial activity of MnO NPs using agar well diffusion method

The antibacterial activity of MnO NPs at concentrations of 50, 100, and 150 µg/ml was tested using the agar well diffusion method (CLSI, 2009a). On Mueller-Hinton agar (MHA) plates, the antibacterial activity against *B. cereus* and *E. coli*, was evaluated. A 0.5 McFarland from each strain was prepared and inoculated on the surface MHA plates using a sterile cotton swap. MnO NPs and Penicillin G (standard antibacterial) were applied aseptically to wells (5 mm) punched into the inoculated agar plates. The agar plates were incubated at 37°C for 24 hrs. After the incubation time, the inhibition zones were measured (mm).

Minimum inhibitory concentration (MIC)

According to the CLSI (2009b), the MIC of MnO NPs *B. cereus* and *E. coli* was determined. Mueller-Hinton broth (MHB) flasks were prepared, inoculated by 0.5 McFarland standard of tested bacteria, supplemented by serial solutions of MnO NPs and Penicillin G (5-50 µg/ml) and incubated at 37°C for 24 hrs. After the incubation time, spectrophotometric measurements of the bacterial growth rates at 600 nm were used to calculate the MIC values.

Minimal microbicidal concentration (MBC)

MBC is the dilution that totally inhibits the formation of microbial colonies on agar plates (Stratton et al., 1982). To find the least bactericidal concentration, subcultures of the tested dilutions that totally prevented the growth of the tested bacteria in the MIC experiment (no visible bacterial growth) were inoculated into the MHA plate using the pour plate technique. The agar plates were incubated at 37°C for 24 hrs.

Statistical analysis

Using SPSS version 18, the results were statistically assessed and evaluated using a one-way analysis of variance (ANOVA) with 0.05 as the significant level.

Results

Biosynthesis of MnO NPs using B. subtilis ATCC6633

B. subtilis ATCC6633 biosynthesize MnO NPs within 2 minutes at 60°C and 200 rpm. The color of the reaction mixture was changed from colorless to dark brown as a primary indicator of the formation of MnO NPs. UV-Vis spectrum showed the successful formation of MnO NPs due to the appearance of two characteristic peaks of MnO at 285 and 353 nm (Figure 1).

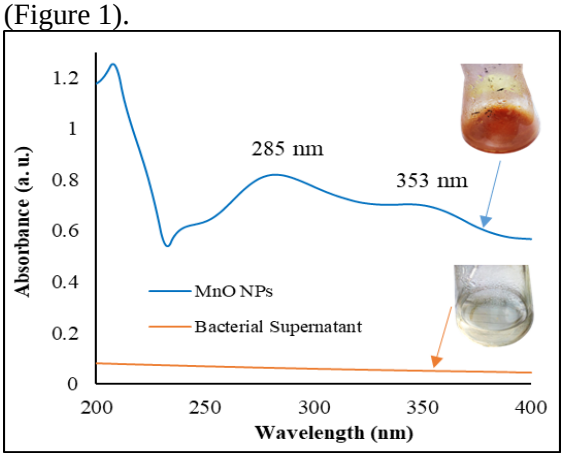

Figure 1. The UV-Vis spectrum and color-change of the reaction mixture during the synthesis of MnO NPs.

Characterization of MnO NPs

FT-IR, Zeta analysis, and TEM were used to characterize the biosynthesized MnO NPs. Proteins were present during the production of MnO NPs, according to the FT-IR spectra (Figure 2). The vibrational frequencies of the stretch, primary, and secondary amines were measured at 3380.1 cm^{-1}, 2917.77 cm^{-1}, and 2337.31 cm^{-1}, respectively.

The stretching vibrations, which are O-H bending vibrations and C-O (hydroxyl, ester, or ether) stretching vibrations, were visible in the bands at 1739.14 cm^{-1} and 1619.91 cm^{-1}. Stretch C-N vibrations were present at 1120.43 cm^{-1} bands in both aromatic and aliphatic amines. The stretching vibration of the Mn-O and Mn-O-Mn bonds, according to Chen and He (2008), showed two prominent peaks at about 630 cm^{-1} and 525 cm^{-1}, which point to MnO production in the current work.

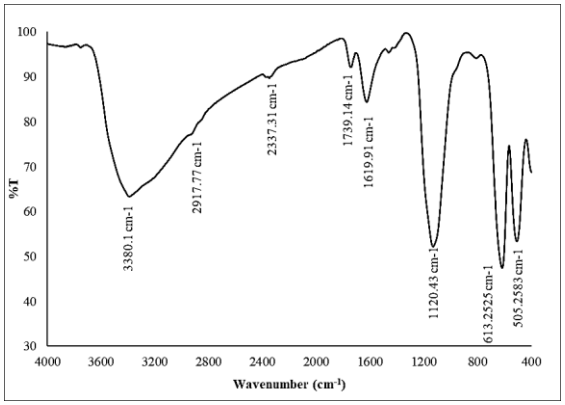

Figure 2. FT-IR spectroscopy of the biosynthesized MnO NPs.

The negative charge of MnO NPs (-20.4 mV) was revealed by zeta analysis results (Figure 3).

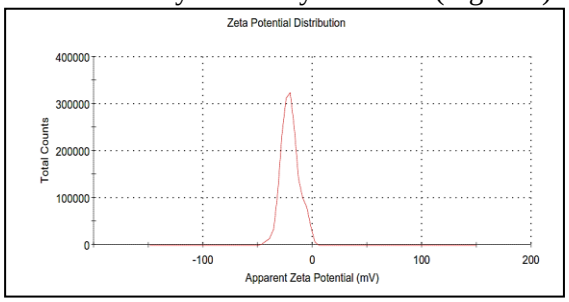

Figure 3. Zeta potential result of MnO NPs.

The nanorod-shaped MnO NPs were formed, and the TEM micrograph corroborated this. The nanorods' lengths and diameters were between 70 and 100 nm and 10 and 23 nm, respectively (Figure 4).

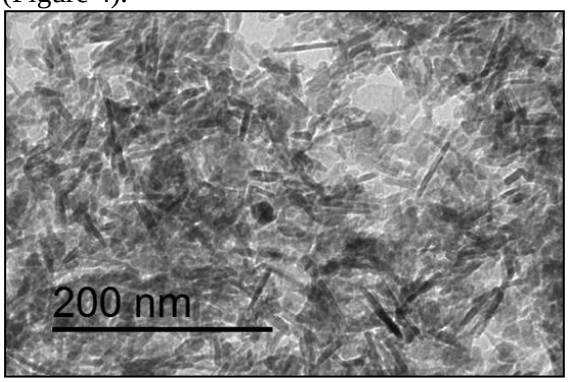

Figure 4. TEM micrographs of MnO NPs (scale bar = 200 nm).

Antibacterial activity of optimized MnO NPs

As indicated in Figure 5 and Table 1, the MnO NPs demonstrated significant antibacterial action against both Gram-negative and Gram-positive bacteria. Gram-negative bacteria were more resistant to MnO NPs' antibacterial effects than Gram-positive bacteria.

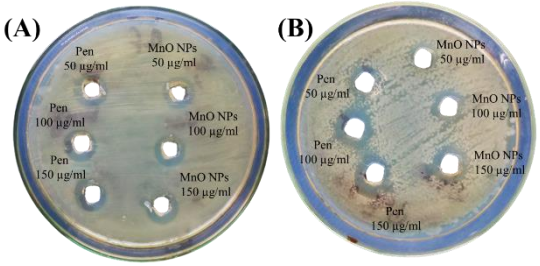

Figure 5. Antibacterial activity of MnO NPs using agar well diffusion method against *B. cereus*; (A) and *E. coli*; (B) compared to penicillin G; (Pen).

Table 1. Antibacterial activity of MnO NPs.

Antibacterial agents	Concentration, µg/ml	Zone of inhibition (mm, mean ± SD, n=3)	
		B. cereus	*E. coli*
MnO NPs	50	18 ± 0.03*	20 ± 0.03*
	100	20 ± 0.03*	23 ± 0.03*
	150	23 ± 0.06*	25 ± 0 *
Penicillin G	50	12 ± 0.06*	27 ± 0*
	100	14 ± 0.06*	30 ± 0*
	150	17 ± 0.03*	33 ± 0*

*Highly significant at $p<0.05$.

The MIC and MBC of MnO NPs against *B. cereus* and *E. coli* were investigated. The most effective concentration to inhibit *B. cereus* and *E. coli* growth was 20 and 15 µg/ml, respectively (Figure 6A). The MBC results confirmed the biocidal action of MnO NPs at the same concentration of MIC values (Figure 6B).

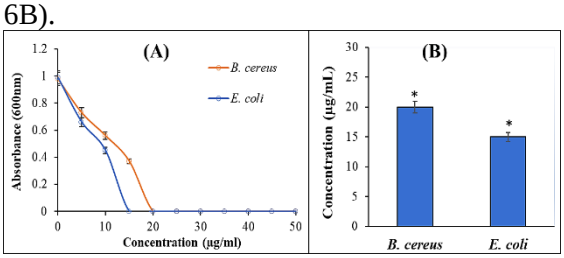

Figure 6. (A) Minimal inhibitory concentration of MnO NPs. (B) Minimal microbicidal concentration of MnO NPs.

Discussion

Mn is a key component in industrial and medicinal applications and is the third most often used metal after iron, aluminium, and copper. Due to its exceptional physical qualities, it can be employed as an ingredient in industrial alloy metals, particularly stainless steel. It is frequently found in minerals. Importantly, Mn is an essential nutrient for both plants and animals and is required for maintaining the structure of chloroplasts in plants. Since it is a vital part of numerous enzymes that support early seedling growth and seed germination in the plant system (Alejandro et al., 2020; Hoseinpour & Ghaemi, 2018), it is significant. In addition, Mn promotes the growth of immunological cells, strengthening an animal's immune system. Additionally, it participates in protein metabolism, stimulates cholesterol synthesis, and aids in the formation and development of human bones (Avila et al., 2013; Silva et al., 2019). In addition to having strong antibacterial characteristics and being less toxic, Mn is regarded as a key component of metabolism and its homeostasis has been successfully regulated by biological systems (Liu et al., 2014; Luo et al., 2004). According to Markides et al. (2012), Masdor et al. (2016), Mo et al. (1998), Nicoloff et al. (2004), and Pi et al. (2016), the Mn^{2+} ions form free radicals that are crucial in the development of clinical illnesses including heart disease, stroke, diabetes mellitus, Alzheimer's, sclerosis, etc.

According to numerous studies (Kumar et al., 2018; Li et al., 2006; Li et al., 2013; Perachiselvi et al., 2020), MnO NPs have numerous benefits due to their low cost, natural abundance due to the existence of Mn in various oxidation states, and effectiveness as catalysts. These applications include biosensors, water treatment, imaging contrast agents, cancer treatment, drug delivery, biomarkers, etc.

The production of nanoscale materials by biological organisms is a promising technique for the synthesis of MnO NPs. It is well known that bacteria can produce inorganic substances both inside and outside of their cells. Bacterial secondary metabolites may reduce Mn salts to the nanoscale range as a bio-reducing agent (Alsaiari et al., 2023). The current study uses a metabolite of *B. subtilis* ATCC6633 to biosynthesize MnO NPs, which are then used as a potent antibacterial agent against both Gram-negative and Gram-positive bacterial strains.

Within 2 min at 60°C with continuous stirring at 200 rpm, *B. subtilis* ATCC6633 could biosynthesize MnO NPs. The stability of NPs is one of the most important factors in determining whether they will work in the pharmaceutical and medical industries. In several investigations, the presence of proteins during the biogenic production of MnO NPs was documented (El-Nour et al., 2023; Fayed et al., 2023). According to El-Dein et al. (2002), these proteins may contribute to the stabilization of NPs by preventing their aggregation and serving as a capping agent. In addition, the surface charge of NPs could help increase their stability by increasing the repulsion force between the particles (Bian et al., 2011). MnO NPs were rod-shaped and negatively charged NPs.

MnO NPs had strong antibacterial activity during the antimicrobial testing. Saod et al. (2022) reported the strong antibacterial activity of MnO NPs against *E. coli* and *P. aeruginosa*, with inhibition zones of 12 and 18 mm, respectively. Also, she reported MIC of the MnO NPs reached 12.5 µg/ml. Compared to Gram-negative bacteria, Gram-positive bacteria were more resistant to MnO NPs. The structure of the cell walls that distinguishes Gram-positive and Gram-negative bacteria is frequently cited as the reason for this disparity in antibacterial action. Because *B. cereus* has a thicker cell wall that blocks the action of MnO NPs, the bacterium is more resistant to the antibacterial activity of MnO NPs, perhaps making it a better defensive system against MnO NPs (Yin et al., 2015). Furthermore, lipopolysaccharides present in Gram-negative bacteria's cell walls give them a higher negative charge than Gram-positive bacteria's, encouraging Mn^{2+} adherence and making the bacteria more vulnerable to the antibacterial activity of released Mn ions (Bonnet et al., 2015). Therefore, the activity of NPs as bactericidal materials depends on the electrostatic interaction between positively charged NPs and negatively charged bacterial cells.

It is widely known that metal oxide NPs have three main mechanisms of action against bacteria: (1) mechanical damage to the cell wall due to electrostatic interaction; (2) oxidative stress due to the production of reactive oxygen species (ROS); and (3) disruption of protein functions and cell structures due to the release of metal cations (Shkodenko et al., 2020).

However, some reported hypotheses claimed that MnO NPs may interact with biological proteins in cell membranes, targeting respiration and cell division, and finally killing cells. The precise antibacterial mechanism of MnO NPs is currently unknown. Additionally, the generation of reactive oxygen species, alterations in cell wall permeability, and other bactericidal effects of MnO NPs have all been documented in several studies (Sirelkhatim et al., 2015).

Additional studies may aid clarification of the MnO NPs' antibacterial mechanism.

Conclusion

The present work presents a green, affordable, and ecologically acceptable technique for the production of MnO NPs using the metabolite *B. subtilis* ATCC6633, which works as an effective reducing and stabilizing agent. The rod-shaped, biosynthesized MnO NPs had lengths of 70 to 100 nm and diameters of 10 to 23 nm. They possessed a negative charge of -20.4 mV. The synthesized MnO NPs successfully suppressed *B. cereus* and *E. coli*. Depending on the concentration of biosynthesized MnO NPs, both Gram-positive and Gram-negative bacteria were severely inhibited.

References

Alejandro, S., Höller, S., Meier, B., & Peiter, E. (2020). Manganese in plants: from acquisition to subcellular allocation. Frontiers in Plant Science, 11, 300.

Ali, H., Khan, E., & Ilahi, I. (2019). Environmental chemistry and ecotoxicology of hazardous heavy metals: environmental persistence, toxicity, and bioaccumulation. Journal of Chemistry, 6730305.

Alsaiari, N. S., Alzahrani, F. M., Amari, A., Osman, H., Harharah, H. N., Elboughdiri, N., & Tahoon, M. A. (2023). Plant and microbial approaches as green methods for the synthesis of nanomaterials: Synthesis, applications, and future perspectives. Molecules, 28(1), 463.

Bar, H., Bhui, D. K., Sahoo, G. P., Sarkar, P., De, S. P., & Misra, A. (2009). Green synthesis of silver nanoparticles using latex of *Jatropha curcas*. Colloids and Surfaces A: Physicochemical and Engineering Aspects, 339(1), 134–139.

Bhattacharya, R., & Mukherjee, P. (2008). Biological properties of "naked" metal nanoparticles. Advanced Drug Delivery Reviews, 60(11), 1289–1306.

Bian S-W, Mudunkotuwa IA, Rupasinghe T, Grassian VH (2011) Aggregation and dissolution of 4 nm ZnO nanoparticles in aqueous environments: influence of pH, ionic strength, size, and adsorption of humic acid. Langmuir, 27: 6059–6068.

Bonnet, M., Massard, C., Veisseire, P. P., Camares, O., & Awitor, K. O. (2015). Environmental toxicity and antimicrobial efficiency of titanium dioxide nanoparticles in suspension. Journal of Biomaterials and Nanobiotechnology, 6(03), 213-224.

Buzea, C., Pacheco, I. I., & Robbie, K. (2007). Nanomaterials and nanoparticles: Sources and toxicity. Biointerphases, 2(4), MR17–MR71.

Chen, H., & He, J. (2008). Facile synthesis of monodisperse manganese oxide nanostructures and their application in water treatment. The Journal of Physical Chemistry C, 112(45), 17540-17545.

Clinical and Laboratory Standards Institute. 2009a. Performance standards for antimicrobial disk susceptibility tests; approved standard M2-A10, 10th ed. Clinical and Laboratory Standards Institute, Wayne, PA.

Clinical and Laboratory Standards Institute. 2009b. Methods for dilution susceptibility tests for bacteria that grow aerobically; approved standard. M7-A8, 8th ed. Clinical and Laboratory Standards Institute, Wayne, PA.

da Silva, A. P. S., Ferreira, B. S., Favarim, H. R., Silva, M. F. F., Silva, J. V. F., dos Anjos Azambuja, M., & Campos, C. I. (2019). Physical properties of medium density fiberboard produced with the addition of ZnO nanoparticles. BioResources, 14(1), 1618–1625.

Dawadi, S., Gupta, A., Khatri, M., Budhathoki, B., Lamichhane, G., & Parajuli, N. (2020). Manganese dioxide nanoparticles: Synthesis, application and challenges. Bulletin of Materials Science, 43, 1–10.

El-Dein MMN, Baka ZA, Abou-Dobara MI, El-Sayed AK, El-Zahed M M (2021) Extracellular biosynthesis, optimization, characterization and antimicrobial potential of *Escherichia coli* D8 silver nanoparticles. Journal of Microbiology, Biotechnology and Food Sciences, 10: 648-656.

El-Nour, A., Amira, T., Abou-Dobara, M. I., El-Sayed, A. K., & El-Zahed, M. M. (2023). Extracellular biosynthesis and antimicrobial activity of *Bacillus subtilis* ATCC 6633 zinc oxide nanoparticles. Scientific Journal for Damietta Faculty of Science, 13(2), 39-47.

El-Zahed, M. M., Abou-Dobara, M. I. ., El-Sayed, A. K., & Baka, Z. A. M. (2022). Ag/SiO_2

nanocomposite mediated by *Escherichia coli* D8 and their antimicrobial potential. Nova Biotechnologica et chimica, 21(1), e1023.

Enríquez-Sánchez, N., Vilchis-Nestor, A. R., Camacho-López, S., Camacho-López, M. A., & Camacho-López, M. (2020). Influence of ablation time on the formation of manganese oxides synthesized by laser ablation of solids in liquids. Optics & Laser Technology, 131, 106418.

Farina, M., Avila, D. S., Da Rocha, J. B. T., & Aschner, M. (2013). Metals, oxidative stress and neurodegeneration: a focus on iron, manganese and mercury. Neurochemistry International, 62(5), 575–594.

Fayed, R., Elnemr, A. M., & El-Zahed, M. M. (2023). Synthesis, characterization, antimicrobial and electrochemical studies of biosynthesized zinc oxide nanoparticles using the probiotic *Bacillus coagulans* (ATCC 7050). Journal of Microbiology, Biotechnology and Food Sciences, e9962.

Gopinath, V., MubarakAli, D., Priyadarshini, S., Priyadharsshini, N. M., Thajuddin, N., & Velusamy, P. (2012). Biosynthesis of silver nanoparticles from *Tribulus terrestris* and its antimicrobial activity: A novel biological approach. Colloids and Surfaces B: Biointerfaces, 96, 69–74.

Grasso, G., Zane, D., & Dragone, R. (2019). Microbial nanotechnology: challenges and prospects for green biocatalytic synthesis of nanoscale materials for sensoristic and biomedical applications. Nanomaterials, 10(1), 11.

Hoseinpour, V., & Ghaemi, N. (2018). Green synthesis of manganese nanoparticles: Applications and future perspective–A review. Journal of Photochemistry and Photobiology B: Biology, 189, 234–243.

Jin, H., Wang, J., Su, D., Wei, Z., Pang, Z., & Wang, Y. (2015). *In situ* cobalt–cobalt oxide/N-doped carbon hybrids as superior bifunctional electrocatalysts for hydrogen and oxygen evolution. Journal of the American Chemical Society, 137(7), 2688–2694.

Kakade, N. (2003). Nanotechnology: new challenges. Electronics, 35, 3–36.

Kannan, N., Selvaraj, S., & Murty, R. V. (2010). Microbial production of silver nanoparticles. Digest Journal of Nanomaterials and Biostructures, 5(1), 135–140.

Khan, N., & Bano, A. (2016a). Modulation of phytoremediation and plant growth by the treatment with PGPR, Ag nanoparticle and untreated municipal wastewater. International Journal of Phytoremediation, 18(12), 1258–1269.

Khan, N., & Bano, A. (2016b). Role of plant growth promoting rhizobacteria and Ag-nano particle in the bioremediation of heavy metals and maize growth under municipal wastewater irrigation. International Journal of Phytoremediation, 18(3), 211–221.

Kumar, S., Kaur, R., Rajput, R., & Singh, M. (2018). Bio pharmaceutics classification system (BCS) class IV drug nanoparticles: Quantum leap to improve their therapeutic index. Advanced Pharmaceutical Bulletin, 8(4), 617.

Li, W., Yuan, J., Shen, X., Gomez-Mower, S., Xu, L., Sithambaram, S., Aindow, M., & Suib, S. L. (2006). hydrothermal synthesis of structure-and shape-controlled manganese oxide octahedral molecular sieve nanomaterials. Advanced Functional Materials, 16(9), 1247–1253.

Li, X., Xu, H., Chen, Z.-S., & Chen, G. (2011). Biosynthesis of nanoparticles by microorganisms and their applications. Journal of Nanomaterials, 2011, 1–16.

Li, L., Seng, K. H., Liu, H., Nevirkovets, I. P., & Guo, Z. (2013). Synthesis of Mn3O4-anchored graphene sheet nanocomposites via a facile, fast microwave hydrothermal method and their supercapacitive behavior. Electrochimica Acta, 87, 801–808.

Liu, M., Wang, Y., Cheng, Z., Zhang, M., Hu, M., & Li, J. (2014). Electrospun Mn_2O_3 nanowrinkles and Mn_3O_4 nanorods: morphology and catalytic application. Applied Surface Science, 313, 360–367.

Luo, J.-D., Wang, Y.-Y., Fu, W.-L., Wu, J., & Chen, A. F. (2004). Gene therapy of endothelial nitric oxide synthase and manganese superoxide dismutase restores delayed wound healing in type 1 diabetic mice. Circulation, 110(16), 2484–2493.

Markides, H., Rotherham, M., & El Haj, A. J. (2012). Biocompatibility and toxicity of magnetic nanoparticles in regenerative medicine. Journal of Nanomaterials, 2012, 13.

Masdor, N. A., Altintas, Z., & Tothill, I. E. (2016). Sensitive detection of *Campylobacter jejuni* using nanoparticles enhanced QCM sensor. Biosensors and Bioelectronics, 78, 328–336.

Mo, C. M., Li, Y. H., Liu, Y. S., Zhang, Y., & Zhang, L. D. (1998). Enhancement effect of photoluminescence in assemblies of nano-ZnO particles/silica aerogels. Journal of Applied Physics, 83(8), 4389–4391.

Narayanan, K. B., & Sakthivel, N. (2010). Biological synthesis of metal nanoparticles by microbes. Advances in Colloid and Interface Science, 156(1–2), 1–13.

Naseri, M. G., Saion, E. Bin, Ahangar, H. A., Hashim, M., & Shaari, A. H. (2011). Synthesis and characterization of manganese ferrite

nanoparticles by thermal treatment method. Journal of Magnetism and Magnetic Materials, 323(13), 1745–1749.

Nicoloff, G., Blazhev, A., Petrova, C., & Christova, P. (2004). Circulating immune complexes among diabetic children. Journal of Immunology Research, 11, 61–66.

Nikam, A. V, Prasad, B. L. V, & Kulkarni, A. A. (2018). Wet chemical synthesis of metal oxide nanoparticles: a review. CrystEngComm, 20(35), 5091–5107.

Omran, B. A. (2020). Fundamentals of Nanotechnology and Nanobiotechnology. In B. A. Omran (Ed.), Nanobiotechnology: A Multidisciplinary Field of Science (pp. 1–36). Springer International Publishing.

Perachiselvi, M., Bagavathy, M. S., Samraj, J. J., Pushpalaksmi, E., & Annadurai, G. (2020). Synthesis and characterization of Mn_3O_4 nanoparticles for biological studies. Appl. Ecol. Environ. Sci., 8(5), 273–277.

Pi, J.-K., Yang, H.-C., Wan, L.-S., Wu, J., & Xu, Z.-K. (2016). Polypropylene microfiltration membranes modified with TiO_2 nanoparticles for surface wettability and antifouling property. Journal of Membrane Science, 500, 8–15.

Pinc, J., Jankovský, O., & Bartůněk, V. (2017). Preparation of manganese oxide nanoparticles by thermal decomposition of nanostructured manganese carbonate. Chemical Papers, 71, 1031–1035.

Raj, B. G. S., Asiri, A. M., Wu, J. J., & Anandan, S. (2015). Synthesis of Mn3O4 nanoparticles via chemical precipitation approach for supercapacitor application. Journal of Alloys and Compounds, 636, 234–240.

Ranjan, M., Bhatnagar, M., & Mukherjee, S. (2015). Localized surface plasmon resonance anisotropy in template aligned silver nanoparticles: A case of biaxial metal optics. Journal of Applied Physics, 117(10), 103106.

Reddy, R. N., & Reddy, R. G. (2003). Sol–gel MnO_2 as an electrode material for electrochemical capacitors. Journal of Power Sources, 124(1), 330–337.

Salavati-Niasari, M., Davar, F., & Mir, N. (2008). Synthesis and characterization of metallic copper nanoparticles via thermal decomposition. Polyhedron, 27(17), 3514–3518.

Saod, W. M., Hamid, L. L., Alaallah, N. J., & Ramizy, A. (2022). Biosynthesis and antibacterial activity of manganese oxide nanoparticles prepared by green tea extract. Biotechnology Reports, 34, e00729.

Shaik, D. P. M. D., Pitcheri, R., Qiu, Y., & Hussain, O. M. (2019). Hydrothermally synthesized porous Mn3O4 nanoparticles with enhanced electrochemical performance for supercapacitors. Ceramics International, 45(2), 2226–2233.

Shkodenko, L., Kassirov, I., & Koshel, E. (2020). Metal oxide nanoparticles against bacterial biofilms: Perspectives and limitations. Microorganisms, 8(10), 1545.

Shukla, S., Jadaun, A., Arora, V., Sinha, R. K., Biyani, N., & Jain, V. K. (2015). *In vitro* toxicity assessment of chitosan oligosaccharide coated iron oxide nanoparticles. Toxicology Reports, 2, 27–39.

Sirelkhatim, A., Mahmud, S., Seeni, A., Kaus, N. H. M., Ann, L. C., Bakhori, S. K. M., ... & Mohamad, D. (2015). Review on zinc oxide nanoparticles: antibacterial activity and toxicity mechanism. Nano-micro Letters, 7(3), 219-242.

Stratton, C. W., Weinstein, M. P., & Reller, L. B. (1982). Correlation of serum bactericidal activity with antimicrobial agent level and minimal bactericidal concentration. Journal of Infectious Diseases, 145(2), 160-168.

Velusamy, P., Kumar, G. V., Jeyanthi, V., Das, J., & Pachaiappan, R. (2016). Bio-inspired green nanoparticles: synthesis, mechanism, and antibacterial application. Toxicological Research, 32, 95–102.

Verma, A. K., Singh, V. P., & Vikas, P. (2012). Application of nanotechnology as a tool in animal products processing and marketing: an overview. American Journal of Food Technology, 7(8), 445–451.

Yang, W., Peng, D., Kimura, H., Zhang, X., Sun, X., Pashameah, R. A., Alzahrani, E., Wang, B., Guo, Z., & Du, W. (2022). Honeycomb-like nitrogen-doped porous carbon decorated with Co_3O_4 nanoparticles for superior electrochemical performance pseudo-capacitive lithium storage and supercapacitors. Advanced Composites and Hybrid Materials, 5(4), 3146–3157.

Yin, R., Agrawal, T., Khan, U., Gupta, G. K., Rai, V., Huang, Y. Y., & Hamblin, M. R. (2015). Antimicrobial photodynamic inactivation in nanomedicine: small light strides against bad bugs. Nanomedicine, 10(15), 2379-2404.

الملخص العربي

عنوان البحث: التصنيع البيولوجي وتوصيف جسيمات أكسيد المنجنيز النانومترية المضادة للبكتيريا باستخدام بكتيريا باسيلس ساتلس (ATCC6633)

عبد الله الزاهد[١]، محمود الحسيني خليفة[١]، محمد مرزوق الزاهد*[١]، زكريا عوض بقا[١]
[١] قسم النبات والميكروبيولوجي، كلية العلوم، جامعة دمياط، مصر

تعد مصادر التصنيع الخضراء للجسيمات النانومترية خاصة أكاسيد المعادن مجالًا بحثيًا مثيرًا للاهتمام ومتوسعًا نظرًا لتطبيقاتها المتعددة كعوامل مضادة للبكتيريا. بشكل عام، يتم تحضير الجسيمات النانومترية باستخدام طرق كيميائية وفيزيائية مختلفة والتي تنتج جسيمات نانومترية سامة أو ضارة، علاوة على التكلفة العالية وخطوات التصنيع المعقدة. نجحت الدراسة الحالية في تصنيع جسيمات أكسيد المنجنيز النانومترية عن طريق اختزال كبريتات المنجنيز باستخدام المستخلص البكتيري الخالي من الخلايا لبكتيريا باسيلس ساتلس (ATCC6633). تم تأكيد تكون جسيمات أكسيد المنجنيز النانومترية بواسطة التحليل الطيفي للأشعة فوق البنفسجية والمرئية، التحليل الطيفي للأشعة تحت الحمراء، تحليل زيتا والمجهر الإلكتروني النافذ. أظهرت جسيمات أكسيد المنجنيز النانومترية المُصنّعة حيويًا منحنيين امتصاص عند ٢٨٥ و٣٥٣ نانومتر. أكد طيف الأشعة تحت الحمراء وجود البروتينات البكتيرية أثناء التصنيع الحيوي لجسيمات أكسيد المنجنيز النانومترية والتي قد تعمل كعوامل تثبيت لها. تمتلك جسيمات أكسيد المنجنيز النانومترية شحنة سالبة تبلغ -٢٠,٤ مللي فولت وفقًا لتحليل زيتا. أظهرت الصور المجهرية الشكل العصوي لجسيمات أكسيد المنجنيز النانومترية بأطوال تتراوح من ٧٠ إلى ١٠٠ نانومتر وأقطار تتراوح من ١٠ إلى ٢٣ نانومتر. كان لجسيمات أكسيد المنجنيز النانومترية تأثيرا مبيدا للجراثيم ضد بكتيريا باسيلس سيريس وإيشيرشيا كولاي مظهرا مناطق تثبيط تبلغ ٢٣ و٢٥ ملم، على التوالي، بالإضافة إلى قيم تركيز التثبيط الأدنى البالغة ٢٠ و١٥ ميكروجرام/مل، على التوالي. تسلط النتائج التي تم الحصول عليها الضوء على إمكانية استخدام جسيمات أكسيد المنجنيز النانومترية كعامل قوي مضاد للبكتيريا في التطبيقات الصناعية والطبية المختلفة.